Solution of the Cox–Thompson inverse scattering problem using finite set of phase shifts

2003 J. Phys. A: Math. Gen. 36 4815

(http://iopscience.iop.org/0305-4470/36/17/308)

INSTITUTE OF PHYSICS PUBLISHING JOURNAL OF PHYSICS A: MATHEMATICAL AND GENERAL

J. Phys. A: Math. Gen. **36** (2003) 4815–4826 PII: S0305-4470(03)57022-6

Solution of the Cox–Thompson inverse scattering problem using finite set of phase shifts

Barnabás Apagyi[1], **Zoltán Harman**[2] **and Werner Scheid**[2]

[1] Department of Theoretical Physics, Budapest University of Technology and Economy, Budapest, Hungary
[2] Institut für Theoretische Physik der Justus-Liebig-Universität, Giessen, Germany

Received 22 November 2002, in final form 4 February 2003
Published 16 April 2003
Online at stacks.iop.org/JPhysA/36/4815

Abstract

A system of nonlinear equations is presented for the solution of the Cox–Thompson inverse scattering problem (1970 *J. Math. Phys.* **11** 805) at fixed energy. From a given finite set of phase shifts for physical angular momenta, the nonlinear equations determine related sets of asymptotic normalization constants and nonphysical (shifted) angular momenta from which all quantities of interest, including the inversion potential itself, can be calculated. As a first application of the method we use input data consisting of a finite set of phase shifts calculated from Woods–Saxon and box potentials representing interactions with diffuse or sharp surfaces, respectively. The results for the inversion potentials, their first moments and asymptotic properties are compared with those provided by the Newton–Sabatier quantum inversion procedure. It is found that in order to achieve inversion potentials of similar quality, the Cox–Thompson method requires a smaller set of phase shifts than the Newton–Sabatier procedure.

PACS numbers: 03.65.Nk, 05.45, 24.10.−i, 25.70.−z

1. Introduction

Although the inverse scattering problem of the Schrödinger operator with central potential has already been solved at fixed energy (see, e.g., [1]), the theory cannot be applied in practice because it requires data which are not accessible by experiments. Some practical theories have therefore been formulated which solve the integral equation of Gel'fand–Levitan–Regge-type with input kernels defined in terms of spectroscopical quantities (i.e. experimentally accessible information such as a set of phase shifts). A successful quantum inversion technique at fixed energy is that introduced by Newton [2] and Sabatier [3] (NS) and modified by Münchow, Scheid and co-workers [4]. This modified NS (mNS) method has been extended into various directions in order to treat, e.g., complex potentials [5, 6] or coupled-channel problems [7].

Another interesting method is suggested by Cox and Thompson (CT) [8, 9] who derived nonlinear equations for solving the inverse scattering problem with a finite dataset at fixed energy. Despite the fact that the theoretical formulation of the CT method dates back to as early as 1970, the difficult problem of constructing equations to be solved by using a finite set of phase shifts is apparently still lacking. The purpose of this work is to fill this gap. Starting from the Povzner–Levitan (PL) representation of the scattering wavefunction and using the asymptotical property of the functions appearing, we set up a system of nonlinear equations for determining the finite set of nonphysical (shifted) angular momenta $\{L_i\}$, $i = 1, 2, \ldots, N$, from which all quantities of interest can be calculated (including the inversion potential itself).

As a first application of the CT method we take finite sets of phase shifts derived from local short range (box and Woods–Saxon) potentials tailored so as to represent situations of interactions with both rigid and diffuse surfaces. By solving the nonlinear equations (using standard root-finding packages [10]) we re-derive the potentials and compare them with the original ones. To draw conclusions also in connection with an alternative inversion method at fixed energy we always calculate potentials by using the NS method. In general, it is found that many more phase shifts are required by the NS procedure, especially at low energies, in order to achieve the same quality in the inversion potentials.

Let us note that this finding reflects the basic differences between the NS and CT methods. The former has been constructed by involving an infinite set of scattering phase shifts. Any truncation of this set which in practice always occurs leads to an inversion potential with vanishing first moment [11] that results in nonphysical oscillation in the asymptotic region. This is contrasted with the CT inversion potential which has in general a finite first moment [8].

A brief review of the CT method is given in section 2. In section 3 we derive nonlinear equations for determining the nonphysical (shifted) angular momenta from a finite set of phase shifts $\{\delta_i\}$, $i = 1, \ldots, N$, with the corresponding physical angular momenta $\{l_i\}$. Section 4 contains illustrative results. The summary and conclusions comprise section 5.

2. Brief review of the Cox–Thompson method

Cox and Thompson (CT) define two disjoint finite sets S and T, each consisting of N distinct real numbers chosen from the interval $\left(-\frac{1}{2}, \infty\right)$. Then they define the input symmetrical kernel as follows:

$$g(r, r') = \sum_{l \in S} \gamma_l u_l(r_<) v_l(r_>) \tag{1}$$

where γ_l are real coefficients, and $u_l(r)$ and $v_l(r)$ are, respectively, the regular Ricatti–Bessel functions $(\pi r/2)^{1/2} J_{l+\frac{1}{2}}(r)$ and the irregular Weber–Schläfli functions $(\pi r/2)^{1/2} Y_{l+\frac{1}{2}}(r)$ [12]. As usual $r_<$ ($r_>$) stands for the lesser (greater) of the distance variables r, r'. The indices l are associated with the physical angular momentum quantum numbers which take integer values ($l = 0, 1, 2, \ldots$) for non-identical particle collisions and even values ($l = 0, 2, 4, \ldots$) for identical particle scattering if the particles are bosons.

The function $g(r, r')$ satisfies the partial differential equation

$$D_0(r) g(r, r') = D_0(r') g(r, r') \tag{2}$$

with the reference Schrödinger operator

$$D_0(r) = r^2 \left(\frac{\partial^2}{\partial r^2} + 1 \right) \tag{3}$$

and boundary conditions

$$g(0, r') = g(r, 0) = 0. \tag{4}$$

Here and in the following, we use atomic units $\hbar^2/2\mu = 0.5$ and first set the wave number $k = 1$.

Now, CT define the transformation kernel $L(r, r')$ as the unique solution of the linear integral equation of Gel'fand–Levitan–Regge-type,

$$L(r, r') = g(r, r') - \int_0^r \mathrm{d}r'' \, r''^{-2} L(r, r'') g(r'', r') \qquad r \geqslant r' \tag{5}$$

with the boundary condition

$$\lim_{r' \to 0} |L(r, r')| r'^{-1/2} = O(1). \tag{6}$$

From the above equations it follows by differentiating and integrating twice by parts, that the transformation kernel satisfies the partial differential equation

$$D(r) L(r, r') = D_0(r') L(r, r') \tag{7}$$

with the Schrödinger operators

$$D(r) = D_0(r) - r^2 V(r) \tag{8}$$

where the (dimensionless) potential is defined by the relation

$$V(r) = -\frac{2}{r} \frac{\mathrm{d}}{\mathrm{d}r} \left(\frac{L(r, r)}{r} \right). \tag{9}$$

Next, CT introduce a PL representation for the regular scattering function with the definition

$$\phi_l(r) = u_l(r) - \int_0^r \mathrm{d}r' \, r'^{-2} L(r, r') u_l(r') \qquad l \in S. \tag{10}$$

Using (7) one readily shows that ϕ_l satisfies the Schrödinger equation

$$D(r) \phi_l(r) = l(l+1) \phi_l(r) \qquad l \in S \tag{11}$$

with the boundary condition $\phi_l(0) = 0$.

To solve the integral equation (5), CT make the ansatz

$$L(r, r') = \sum_{L \in T} A_L(r) u_L(r') \tag{12}$$

where not only the functions $A_L(r)$ but also the real numbers $L \in T$ have to be determined. A stringent condition here is that the sets S and T, both consisting of N elements, should be disjoint.

Insertion of the ansatz (12) into equation (5) and using the linear independence of the functions $u_m(r)$, $m \in S \cup T$, one arrives at two separate, though coupled, sets of equations for the expansion coefficients γ_l and the expansion functions $A_L(r)$. The first set of equations is

$$\sum_{l \in S} \frac{\gamma_l}{l(l+1) - L(L+1)} = 1 \qquad L \in T \tag{13}$$

from which the expansion coefficients γ_l can be obtained [9] as

$$\gamma_l = \frac{\prod_{L \in T} [l(l+1) - L(L+1)]}{\prod_{l' \in S, l' \neq l} [l(l+1) - l'(l'+1)]} \qquad l \in S. \tag{14}$$

The second set of equations reads

$$\sum_{L\in T} A_L(r)\frac{W[u_L(r), v_l(r)]}{l(l+1)-L(L+1)} = v_l(r) \qquad l \in S \tag{15}$$

where the Wronskian is defined by $W[a(x), b(x)] \equiv a(x)b'(x) - a'(x)b(x)$, and the unknown functions $A_L(r)$ appear linearly, but the numbers $L \in T$ occur in a highly nonlinear manner. As expected, it will turn out that the numbers $L \in T$ play the role of some sort of nonphysical (shifted or generalized) angular momenta.

Apparently the above CT equations (15) have not yet been solved for any particular problem. One reason may be because of the nonlinear character of the equations. In the next section these equations will be solved using a set of phase shifts $\{\delta_l\}$, $l \in S$, as input data.

3. Nonlinear equations

In order to carry out an explicit calculation of the CT method, we use the asymptotic properties of the functions

$$u_l(r \to \infty) = \sin(r - l\pi/2) \tag{16}$$

$$v_l(r \to \infty) = -\cos(r - l\pi/2) \tag{17}$$

$$\phi_l(r \to \infty) = B_l \sin(r - l\pi/2 + \delta_l) \tag{18}$$

where the numbers $\{B_l\}$, $l \in S$, mean the unknown normalizing constant and the set $\{\delta_l\}$, $l \in S$, denotes the input phase shifts. Of course, the set of equations (15) alone is not sufficient to determine the functions $A_L(r)$ because the numbers L also appear explicitly in the denominator. Therefore, we use another set of equations, namely the Povzner–Levitan representation (10) for the regular wavefunction. This also allows the input phase shifts to enter the inversion procedure. Then we determine both the functions $A_L(r)$ and the set of numbers $L \in T$.

Using formulae (16), (18), and the ansatz (12), the PL representation (10) can be written formally for $r \to \infty$ as

$$B_l \sin(r - l\pi/2 + \delta_l) = \sin(r - l\pi/2) - \sum_{L\in T} A_L(r \to \infty) \int_0^\infty \mathrm{d}r'\, r'^{-2} u_L(r') u_l(r') \qquad l \in S. \tag{19}$$

The last integral can easily be evaluated and we get

$$B_l \sin(r - l\pi/2 + \delta_l) = \sin(r - l\pi/2) + \sum_{L\in T} A_L(r \to \infty)\frac{\sin[(l-L)\pi/2]}{L(L+1) - l(l+1)} \qquad l \in S. \tag{20}$$

Now, equation (15) will be applied to determine the asymptotic form of A_L. To this end we use formulae (16), (17) and write equation (15) at the asymptotic limit $r \to \infty$ to be

$$\sum_{L\in T} A_L(r \to \infty)\frac{\cos[(l-L)\pi/2]}{l(l+1) - L(L+1)} = -\cos(r - l\pi/2) \qquad l \in S. \tag{21}$$

By inversion, the asymptotic form of A_l can be obtained as

$$A_L(r \to \infty) = \sum_{l'\in S} K_{Ll'} \cos(r - l'\pi/2) \qquad L \in T \tag{22}$$

with the inverse matrix $K \equiv M^{-1}$ calculated from the matrix M defined by the elements

$$M_{lL} = -\frac{\cos[(l-L)\pi/2]}{l(l+1)-L(L+1)} \qquad l \in S \quad L \in T. \tag{23}$$

Inserting equation (22) into equation (20), one obtains one set of N equations for two sets of $2N$ unknowns, namely $\{L\} \in T$ and $\{B_l\}, l \in S$. This set of N equations can be written in the form ($l \in S$)

$$\begin{aligned}\left[\frac{B_l}{2\mathrm{i}}\,\mathrm{e}^{\mathrm{i}(\delta_l - l\pi/2)} - \frac{1}{2\mathrm{i}}\,\mathrm{e}^{-\mathrm{i}l\pi/2} - \frac{1}{2}\sum_{L\in T}\frac{\sin[\pi(l-L)/2]}{L(L+1)-l(l+1)}\sum_{l'\in S}K_{Ll'}\,\mathrm{e}^{-\mathrm{i}l'\pi/2}\right]\mathrm{e}^{\mathrm{i}r} \\ + \left[-\frac{B_l}{2\mathrm{i}}\,\mathrm{e}^{-\mathrm{i}(\delta_l - l\pi/2)} + \frac{1}{2\mathrm{i}}\,\mathrm{e}^{\mathrm{i}l\pi/2}\right. \\ \left. - \frac{1}{2}\sum_{L\in T}\frac{\sin[\pi(l-L)/2]}{L(L+1)-l(l+1)}\sum_{l'\in S}K_{Ll'}\,\mathrm{e}^{\mathrm{i}l'\pi/2}\right]\mathrm{e}^{-\mathrm{i}r} = 0.\end{aligned} \tag{24}$$

Because of the linear independence of the functions $\mathrm{e}^{\mathrm{i}r}$ and $\mathrm{e}^{-\mathrm{i}r}$, the coefficients in parentheses must vanish so that one arrives at the following two separate sets of N equations ($l \in S$):

$$\frac{B_l}{2\mathrm{i}}\,\mathrm{e}^{-\mathrm{i}l\pi/2}\,\mathrm{e}^{\mathrm{i}\delta_l} = \frac{1}{2\mathrm{i}}\,\mathrm{e}^{-\mathrm{i}l\pi/2} + \frac{1}{2}\sum_{L\in T}\frac{\sin[\pi(l-L)/2]}{L(L+1)-l(l+1)}\sum_{l'\in S}K_{Ll'}\,\mathrm{e}^{-\mathrm{i}l'\pi/2} \tag{25}$$

and

$$-\frac{B_l}{2\mathrm{i}}\,\mathrm{e}^{\mathrm{i}l\pi/2}\,\mathrm{e}^{-\mathrm{i}\delta_l} = -\frac{1}{2\mathrm{i}}\,\mathrm{e}^{\mathrm{i}l\pi/2} + \frac{1}{2}\sum_{L\in T}\frac{\sin[\pi(l-L)/2]}{L(L+1)-l(l+1)}\sum_{l'\in S}K_{Ll'}\,\mathrm{e}^{\mathrm{i}l'\pi/2}. \tag{26}$$

As we see these equations represent an equation and its conjugate in the case of real potentials because the phase shifts δ_l are then real and the norms B_l can also be taken to be real numbers. In this case the above two equations can be written as a single one as follows ($l \in S$):

$$B_l\,\mathrm{e}^{\mathrm{i}(\delta_l - l\pi/2)} = \mathrm{e}^{-\mathrm{i}l\pi/2} + \sum_{L\in T, l'\in S}\frac{\sin[\pi(l-L)/2]}{L(L+1)-l(l+1)}K_{Ll'}\,\mathrm{e}^{\mathrm{i}(1-l')\pi/2} \tag{27}$$

whose real part gives ($l \in S$)

$$B_l\cos(\delta_l - l\pi/2) = \cos(l\pi/2) + \sum_{L\in T, l'\in S}K_{Ll'}\frac{\sin(l'\pi/2)\sin[\pi(l-L)/2]}{L(L+1)-l(l+1)} \tag{28}$$

and the imaginary part takes the form ($l \in S$)

$$B_l\sin(\delta_l - l\pi/2) = -\sin(l\pi/2) + \sum_{L\in T, l'\in S}K_{Ll'}\frac{\cos(l'\pi/2)\sin[\pi(l-L)/2]}{L(L+1)-l(l+1)}. \tag{29}$$

Thus the CT theory could be formulated in terms of two sets of nonlinear equations whose solution gives the normalization constants $B_l, l \in S$ and the generalized (nonphysical or shifted) angular momentum quantum numbers $L \in T$ which, in turn, determine the inversion potential (9).

If one is not interested in the normalization constants ($B_l, l \in S$) then one may divide the two equations (28) and (29) by each other to arrive at a system of N nonlinear equations ($l \in S$)

$$\cot(\delta_l - l\pi/2) = \frac{\cos(l\pi/2) + \sum_{L\in T, l'\in S}K_{Ll'}\frac{\sin(l'\pi/2)\sin[\pi(l-L)/2]}{(L(L+1)-l(l+1))}}{-\sin(l\pi/2) + \sum_{L\in T, l'\in S}K_{Ll'}\frac{\cos(l'\pi/2)\sin[\pi(l-L)/2]}{(L(L+1)-l(l+1))}} \tag{30}$$

or

$$\tan(\delta_l - l\pi/2) = \frac{-\sin(l\pi/2) + \sum_{L\in T, l'\in S} K_{Ll'} \frac{\cos(l'\pi/2)\sin[\pi(l-L)/2]}{L(L+1)-l(l+1)}}{\cos(l\pi/2) + \sum_{L\in T, l'\in S} K_{Ll'} \frac{\sin(l'\pi/2)\sin[\pi(l-L)/2]}{L(L+1)-l(l+1)}} \tag{31}$$

where only the set $L \in T$ appears as unknown and the set $\{\delta_l\}, l \in S$, represents the input data. Finding the generalized angular momentum quantum numbers $L \in T$ from the above equations, the inversion potential (9) can be obtained by making use of equations (12) and (15).

Sets of equations (28) and (29), or (30), or (31) represent three possibilities for the solution of the CT method with input phase shifts. In obtaining the numerical results presented in the next section we have found that the application of the Newton–Raphson root-finding procedures [10] is sufficient to solve equation (31). However, there may be cases encountered especially in the case of measured data with some errors when the use of other solution methods, such as the secant method of Broyden [13] or the simulating annealing method [14] or their combination, is necessary. In such cases also employment of other forms of the nonlinear equations (28), (29) or (30) may prove useful in finding the numbers $L \in T$ of shifted angular momenta.

A practical method for finding the numbers L can be obtained by analysing equation (31) for the case $N = 1$, that is when only one angular momentum quantum number plays a role. Such a situation occurs, for example, at low energy which is dominated by the s-wave ($l = 0$) scattering or for resonance scattering, when a particular angular momentum l dominates the cross section. For one input phase shift δ_l, equation (31) can be written in the form

$$\tan(\delta_l - l\pi/2) = \frac{-\sin(l\pi/2)\cos[(l-L)\pi/2] + \cos(l\pi/2)\sin[(l-L)\pi/2]}{+\cos(l\pi/2)\cos[(l-L)\pi/2] + \sin(l\pi/2)\sin[(l-L)\pi/2]} \tag{32}$$

from which the shifted angular momentum readily follows to be

$$L = l - \frac{2}{\pi}\delta_l \tag{33}$$

where the periodicity of L arising from the trigonometric functions has been absorbed by the $n\pi$ ambiguity of the scattering phase shifts δ_l. (It is easy to see that the latter ambiguity does not affect the results (30)–(31) because of the appearance of the normalization constant B_l in equations (18)–(20), and (24)–(29).)

From the above equation (33) we also see that for high angular momentum quantum numbers l when the potential does not play a decisive role (and the phase shifts δ_l tend to zero), the shifted angular momentum quantum numbers L approach the physical ones l. In the following we shall therefore adopt equation (33) as a physically reasonable normalization condition of the numbers L at high l.

One may thus proceed successively to solve equation (31) first with one term ($N = 1$) giving input data l_1, δ_{l_1} and a starting guess $L_1 \sim l_1 - 2\delta_{l_1}/\pi$, then let a nonlinear solver find the correct value of L_1 (which should be $l_1 - 2\delta_{l_1}/\pi$). We then proceed to $N = 2$ by giving additional input data l_2, δ_{l_2} and initial values L_1 (just determined) and $L_2 \sim l_2 - 2\delta_{l_2}/\pi$, and again let the numerical procedure determine both $L_i, i = 1, 2$, simultaneously. At $N = 3$ we give the additional input data l_3, δ_{l_3} and starting values L_1, L_2 (as determined at level $N = 2$), and $L_3 \sim l_3 - 2\delta_{l_3}/\pi$, then let the solver perform the calculation for the correct solutions $L_i, i = 1, 2, 3$. By repeating this procedure one may calculate the wanted set $L \in T$ and then the inversion potential. Let us note that the above procedure can also be used backwards, by starting at the maximal angular momentum $l_N = l_{\max}$ as the first step where the initial L_N is close to l_N, then going downwards until L_1 has been determined with the input data $l_1 = 0$

and δ_0. This latter procedure is useful when the coupling generated by the unknown potential among the L_i is so strong that it is hard to find the appropriate starting values for the lower L_i.

4. Results

All the above formulae have been derived for the case of wave number $k = 1$ by using atomic units ($\hbar^2/2\mu = 0.5$). For the case $k \neq 1$ we obtain the potentials $U(r)$ (possessing a dimension of energy) as follows ($\rho = kr$)

$$U(r) = U\left(\frac{\rho}{k}\right) = EV(\rho) \tag{34}$$

where $E = \hbar^2 k^2/(2\mu)$ and $V(\rho)$ is taken from equation (9).

We also calculate the first moment Q_1 of the CT inversion potential by using the formula [8]

$$Q_1 = \int_0^\infty \mathrm{d}r\, rU(r) = \sum_{L\in T} b_L \tag{35}$$

where the numbers b_L, $L \in T$ are solutions of the system of equations

$$\sum_{L\in T} G_{lL} b_L = -1 \qquad l \in S \tag{36}$$

with the matrix $G_{lL} = 1/(L - l)$. These solutions can also be given explicitly as [8]

$$b_L = \frac{\prod_{l\in S}(L-l)}{\prod_{L'\neq L\in T}(L-L')}. \tag{37}$$

We may also calculate the value of the potential at the origin by applying a power expansion to the Bessel function appearing in equations (12) and (15) with respect to r up to the fourth order, and then by inserting the result into equation (9) to obtain

$$U(0) = E\left(Q - 2(1-Q)\sum_{L\in T, l\in S} (G^{-1})_{Ll}/(1-2l)\right) \tag{38}$$

where

$$Q = \sum_{L\in T} b_L/(L+3/2). \tag{39}$$

In the following subsections where the results will be presented for synthetic data related to Woods–Saxon and box potentials we also list the expansion coefficients γ_l which are determined by the system of equations (13) and given explicitly by equation (14). The coefficients γ_l provide information about the convergence property of the CT ansatz (1).

4.1. WS potential

Figure 1 summarizes the results obtained for the case of $N = 13$ input phase shifts ($l = 0, 1, \ldots, 12$) derived from the Woods–Saxon potential

$$U_{\mathrm{WS}}(r) = \frac{-1}{1+\exp((r-1)/0.25)} \tag{40}$$

at $k = 6$ au. In figure 1 the CT inversion potential is shown by the solid curve and, for comparison, the dashed curve represents the NS inversion potential with the same set of input phase shifts. The superiority of the CT results is obvious, especially at the origin and large distances. We note that such a good quality of results (see also figure 2), except at the origin,

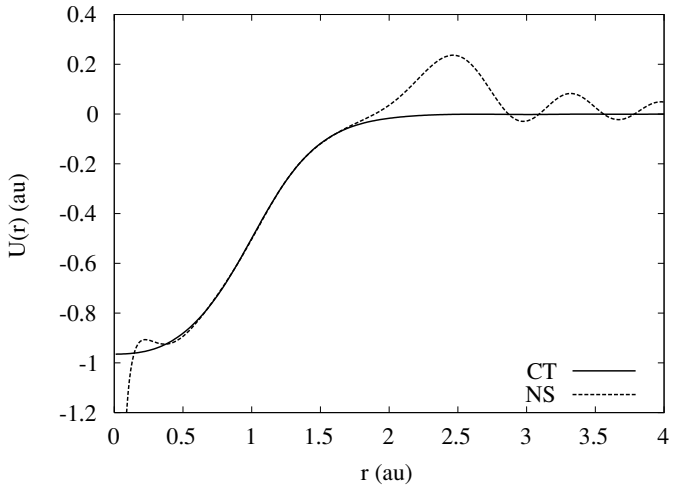

Figure 1. CT inversion potential (solid curve) obtained from (34) as compared to NS results (dashed curve) for the WS potential given by equation (40) at $k = 6$ (au) and $l_{\max} = 12$ ($N = 13$) as a function of the radial distance r.

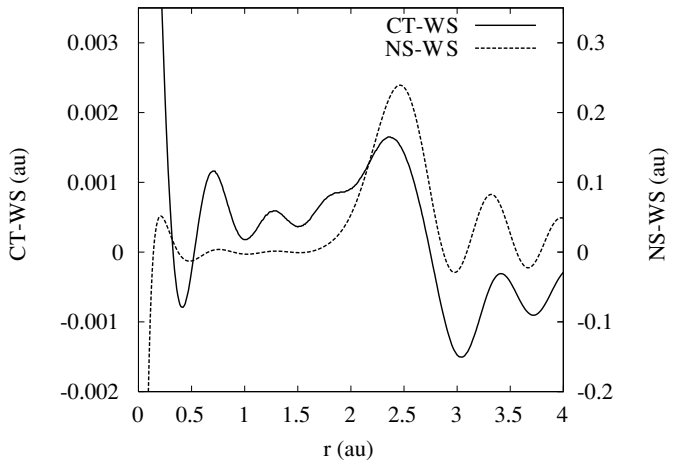

Figure 2. Differences between the CT and WS potentials (solid line) and between the NS and WS potentials (dashed curve). Note the different scale of magnitude on the ordinates on both sides.

can also be obtained by using the NS method if we employ an input set of phase shifts as large as $N \sim 50$ (and take the matching radius not larger than about 8 au when calculating phase shifts back from the NS potential).

In order to exhibit the quality of the CT method more sensibly, we show in figure 2 the differences between the CT and WS potentials as the solid curve, together with the differences between the NS and WS potentials by the dashed curve. Figure 2 clearly shows the similarity of the two inversion methods but on a different scale, differing by two orders of magnitude in favour of the CT method.

Table 1 contains the shifted angular momentum quantum numbers $L_i, i = 1, \ldots, 13$, and expansion coefficients $\gamma_i, i = 1, \ldots, 13$, obtained, respectively, by solving the system of nonlinear equations (31) and by using equation (14). Also listed are the input sets of physical

Table 1. Results for the inversion with WS data. Index number i, shifted angular momentum L_i obtained by solving equation (31), input physical angular momentum l_i, expansion coefficients γ_i calculated by equation (14), input phase shifts $\delta_{l_i}^{\mathrm{WS}}$, output phase shifts $\delta_{l_i}^{\mathrm{CT}}$ generated by CT inversion potential, output phase shifts $\delta_{l_i}^{\mathrm{NS}}$ generated by NS inversion potential shown in figure 1.

i	L_i	l_i	γ_i	$\delta_{l_i}^{\mathrm{WS}}$	$\delta_{l_i}^{\mathrm{CT}}$	$\delta_{l_i}^{\mathrm{NS}}$
1	−0.1297	0	0.0779	0.1654	0.1650	0.1365
2	0.8904	1	0.2586	0.1602	0.1602	0.1304
3	1.9041	2	0.4285	0.1490	0.1490	0.1202
4	2.9182	3	0.5557	0.1322	0.1321	0.1014
5	3.9343	4	0.6077	0.1094	0.1094	0.0800
6	4.9513	5	0.5691	0.0830	0.0829	0.0502
7	5.9670	6	0.4627	0.0575	0.0575	0.0269
8	6.9794	7	0.3341	0.0369	0.0368	0.0011
9	7.9880	8	0.2190	0.0223	0.0222	−0.0111
10	8.9934	9	0.1325	0.0129	0.0129	−0.0268
11	9.9967	10	0.0738	0.0073	0.0072	−0.0341
12	10.9985	11	0.0364	0.0040	0.0040	−0.0409
13	11.9995	12	0.0141	0.0022	0.0021	−0.0704

angular momentum quantum numbers $\{l_i\}$ and phase shifts $\left\{\delta_{l_i}^{\mathrm{WS}}\right\}$ and the sets of phase shifts $\left(\left\{\delta_{l_i}^{\mathrm{CT}}\right\}\right.$ and $\left.\left\{\delta_{l_i}^{\mathrm{NS}}\right\}\right)$ of the inverse potentials resulting from the CT and NS methods, respectively.

Studying table 1 we clearly see the superiority of the CT method. The reproduced phase shifts $\delta_{l_i}^{\mathrm{CT}}$ are very close to the input ones $\delta_{l_i}^{\mathrm{WS}}$ over the whole domain of input angular momentum quantum numbers l_i, $i = 1, \ldots, 13$. Also we observe that the expansion coefficients γ_i are gradually decreasing for large angular momenta while they are nearly constant in the middle range of the expansion domain considered. The shifted angular momenta L_i are gradually approaching their counterparts of physical angular momenta l_i at large quantum numbers while they depart from them at low values of l_i. We may conclude that a large part of the information about the inversion potential is encoded in the differences $L_i - l_i$, $i = 1, \ldots, 13$.

The result for the first moment is $Q_1 = -0.609$ au to be compared to the exact value of -0.601 au. The value of the potential at the origin is $U_{\mathrm{CT}}(0) = -0.965$ au to be compared to $U_{\mathrm{WS}}(0) = -0.982$ au. The respective quantities for the NS method are $Q_1 = 0$ au and $U_{\mathrm{NS}}(0) = -\infty$.

4.2. Box potential

In order to explore the capability of the CT method we have investigated the square-well (box) potential case too. It is well known that this potential represents a sensible test for numerics. Figure 3 shows the results of the CT method (dashed curve) with $k = 6$ au obtained for the box potential

$$U_{\mathrm{BX}}(r) = \begin{cases} -1 & 0 < r < 1 \\ 0 & r > 1. \end{cases} \tag{41}$$

For the input phase shifts we used $N = 8$ and $l_{\max} = 7$. For comparison we have included the inversion potential given by the NS method (dot-dashed curve) with the same size of input set of phase shifts, and the original potential (solid line).

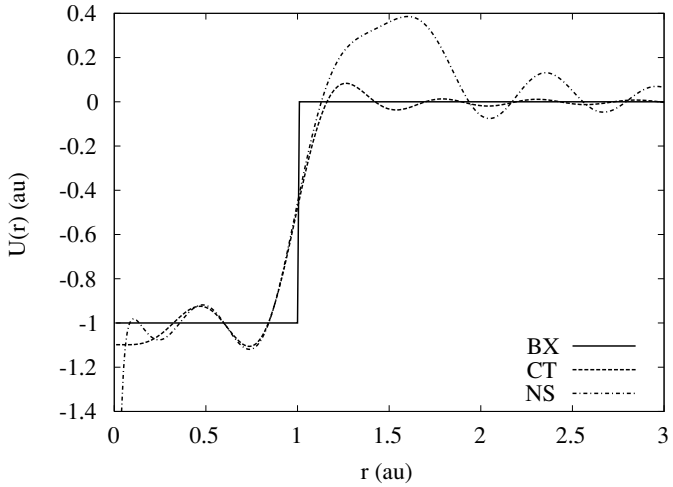

Figure 3. CT inversion potential (dashed curve) obtained from (34) as compared to NS results (dot-dashed curve) for the box potential given by equation (41) (solid line) at $k = 6$ (au) and $l_{\max} = 7$ ($N = 8$) as a function of the radial distance r.

Table 2. Results for the inversion with box potential data. Index number i, shifted angular momentum L_i obtained by solving equation (31), input physical angular momentum l_i, expansion coefficients γ_i calculated by equation (14), input phase shifts $\delta_{l_i}^{\mathrm{BX}}$, output phase shifts $\delta_{l_i}^{\mathrm{CT}}$ and $\delta_{l_i}^{\mathrm{NS}}$ generated from CT and NS inversion potentials, respectively (see figure 3).

i	L_i	l_i	γ_i	$\delta_{l_i}^{\mathrm{BX}}$	$\delta_{l_i}^{\mathrm{CT}}$	$\delta_{l_i}^{\mathrm{NS}}$
1	−0.1309	0	0.0807	0.1676	0.1681	0.1263
2	0.8904	1	0.2667	0.1611	0.1601	0.1216
3	1.9089	2	0.4155	0.1405	0.1413	0.0985
4	2.9047	3	0.6744	0.1547	0.1537	0.1116
5	3.9373	4	0.6243	0.1085	0.1092	0.0634
6	4.9780	5	0.2723	0.0427	0.0420	−0.0093
7	5.9963	6	0.0530	0.0107	0.0111	−0.0411
8	7.0010	7	−0.0167	0.0019	0.0016	−0.0892

In general, one observes for both inversion methods a less satisfactory reproduction compared to the WS potential case. However, the CT method also provides in this case a good result although the performance is poorer than in the WS case, as can also be recognized from table 2. This poorer reproduction can be attributed to the smaller set of input data than that used in the WS case.

In order to test the stability of the numerical method used with respect to possible errors in data we have also performed calculations with slightly changed input phase shifts. The procedure proved to be stable in that a few per cent modification in data induced a negligible difference of values of the inversion potential within the whole spatial domain of interest.

Table 2 contains the shifted angular momentum quantum numbers $L_i, i = 1, \ldots, 8$, and the expansion coefficients $\gamma_i, i = 1, \ldots, 8$, obtained, respectively, by solving the system of nonlinear equations (31) and using equation (14). Also listed are the input sets of physical angular momentum quantum numbers $\{l_i\}$ and phase shifts $\left\{\delta_{l_i}^{\mathrm{BX}}\right\}$ and the sets of phase shifts $\left\{\delta_{l_i}^{\mathrm{CT}}\right\}$ and $\left\{\delta_{l_i}^{\mathrm{NS}}\right\}$ given by the inverse potentials of the CT and NS methods.

The result for the first moment is $Q_1 = -0.51$ au to be compared to the exact value of -0.50 au. The value of the potential at the origin is $U_{\mathrm{CT}}(0) = -1.09$ au to be compared to $U_{\mathrm{BX}}(0) = -1.00$ au. The respective quantities for the NS method are $Q_1 = 0$ au and $U_{\mathrm{NS}}(0) = -\infty$.

5. Summary and conclusion

We have implemented the Cox–Thompson (CT) inverse scattering method to derive potentials from finite sets of phase shifts. By starting with a Povzner–Levitan representation of the regular wavefunction of the CT theory we have shown how a set of nonlinear equations can be constructed for the calculation of the unknown normalization constants and the nonphysical (shifted) angular momenta $\{L_i\}, i = 1, \ldots, N$, which are quantities of central importance in the CT theory. By solving the nonlinear equations (31) with finite sets of phase shifts as input data, we have obtained the sets of the shifted angular momenta $\{L_i\}, i = 1, \ldots, N$, from which we have further calculated various quantities of interest such as the (dimensionless) inversion potential $V(r)$ itself, defined by equation (9), the first moment $\int_0^\infty rU(r)\,\mathrm{d}r$, the potential value at the origin $U(0)$ and the expansion coefficients $\{\gamma_i\}, i = 1, \ldots, N$. To calculate these quantities we have solved simple linear equations (e.g. (15)) or evaluated analytical formulae (such as, e.g., (14), (12), (35), (38)), all containing the pre-determined nonphysical (shifted) angular momenta $\{L_i\}, i = 1, \ldots, N$. It is observed that a large amount of the information on the potentials is encoded in the differences $\{L_i - l_i\}, i = 1, \ldots, N$, between the physical and nonphysical (shifted) angular momenta.

As a first application of the CT method we have chosen finite sets of phase shifts belonging to known potentials of short range type with both sharp and diffuse edges. For both types of potentials we have found that the CT method requires a small set of phase shifts with appreciable magnitude. At a given computer accuracy, the inclusion of smaller phase shifts does not improve the results neither at the origin nor at asymptotical distances. This means that the behavior of the potential at smaller and larger distances is properly accounted for by the CT ansatz (1). This is to be contrasted to the situation produced by the NS method where it can generally be observed that the more phase shifts (even zero ones) are included in the procedure, the better the results. This improvement in the NS method is observed in shifting the singularity of the NS potential closer to the origin, and pushing the nonphysical oscillations towards asymptotical distances.

The quality of the CT inversion potential and the amount of information required by it to generate the potential is similar to those exhibited by the mNS method [4] which assumes a known (prescribed) asymptotics beyond a finite distance r_0. Although the theoretical analysis of a possible connection between the mNS and CT methods remains to be done, the CT method has the advantage that it does not require a stability analysis with respect to changing r_0 (because it has no such free parameter). The price we have to pay in the CT method is the solving of nonlinear equations. In our exploratory calculations we have found that algorithms working on the basis of Newton–Raphson root-finding techniques [10] are sufficient, but there have also been cases encountered when other procedures such as the secant method of Broyden [13] or the simulating annealing method [14] or their combinations have proved successful in finding the numbers $\{L_i\}, i = 1, \ldots, N$, of shifted angular momenta.

Finally, we should note that the CT method deserves to be analysed further and extended into various directions such as, e.g., to include the treatment of Coulomb potentials or complex valued interactions. It would also be interesting to explore the gain which might be expected when the equations are solved with the finite distance r_0 beyond which a prescribed asymptotics of the potential is accurate. Such investigations are in progress.

Acknowledgment

This work is supported by OTKA under grant nos T029884 and T038191.

References

[1] Levitan B M 1987 *Inverse Sturm–Liouville Problems* (Utrecht: VNU Science Press)
[2] Newton R G 1962 *J. Math. Phys.* **3** 75
[3] Sabatier P C 1966 *J. Math. Phys.* **7** 1515
[4] Münchow M and Scheid W 1980 *Phys. Rev. Lett* **44** 1299
[5] May K E, Münchow M and Scheid W 1984 *Phys. Lett.* B **141** 1
[6] Apagyi B, Schmidt A, Scheid W and Voit H 1994 *Phys. Rev.* C **49** 2608
[7] Eberspächer M, Apagyi B and Scheid W 1996 *Phys. Rev. Lett.* **77** 1921
[8] Cox J R and Thompson K W 1970 *J. Math. Phys.* **11** 805
[9] Cox J R and Thompson K W 1970 *J. Math. Phys.* **11** 815
[10] Press W H, Teukolsky S A, Vetterling W T and Flannery B P 1992 *Numerical Recipes* (Cambridge: Cambridge University Press)
[11] Newton R G 1967 *J. Math. Phys.* **8** 1566
[12] Watson G N 1944 *Theory of Bessel Functions* (Cambridge: Cambridge University Press)
[13] Broyden C G 1965 *Math. Comput.* **3** 577
[14] Metropolis N, Rosenbluth A, Rosenbluth M, Teller A and Teller E 1955 *J. Chem. Phys.* **21** 1087